Decreased CCN3 in Systemic Sclerosis Endothelial Cells Contributes to Impaired Angiogenesis

Pauline Henrot, François Moisan, Paôline Laurent, Pauline Manicki, Priscilla Kaulanjan-Checkmodine, Valérie Jolivel, Hamid Reza Rezvani, Vaianu Leroy, François Picard, Carine Boulon, et al.

Decreased CCN3 in Systemic Sclerosis endothelial cells contributes to impaired angiogenesis

Pauline Henrot[1,2], François Moisan[1], Paôline Laurent[3], Pauline Manicki[2,3], Priscilla Kaulanjan-Checkmodine[1], Valérie Jolivel[3], Hamid Reza Rezvani[1,4], Vaianu Leroy[4], François Picard[5], Carine Boulon[6], Thierry Schaeverbeke[2], Julien Seneschal[1,4], Estibaliz Lazaro[3,7], Alain Taïeb[1,4], Marie-Elise Truchetet[2,3]*, and Muriel Cario[1,4]*

* contributed equally to this work

ORCiD IDs: Pauline Henrot: 0000-0002-6528-6092, François Moisan: 0000-0003-2680-7497, Paôline Laurent: 0000-0001-5906-2191, Pauline Manicki: 0000-0001-6573-103X, Priscilla Kaulanjan-Checkmodine: 0000-0002-3708-6165, Valérie Jolivel: 0000-0002-4114-4559, Hamid Rezvani: 0000-0001-8067-1338, Vaianu Leroy: 0000-0002-6228-9271, François Picard: 0000-0003-4426-940X, Carine Boulon: 0000-0002-5508-8906, Thierry Schaeverbeke: 0000-0002-6976-643X, Julien Seneschal: 0000-0003-1139-0908, Estibaliz Lazaro: 0000-0002-4206-7399, Alain Taïeb: 0000-0002-0928-8608, Marie-Elise Truchetet: 0000-0001-8045-0180, Muriel Cario: 0000-0003-0462-5684

1. Univ. Bordeaux, Inserm, BMGIC, UMR1035, 146 rue Léo Saignat, 33 076 Bordeaux, France
2. Department of Rheumatology, National Reference Center for Systemic Autoimmune Rare Diseases, Hopital Pellegrin, place Amélie Raba-Léon, 33 000 Bordeaux, France
3. Univ. Bordeaux, CNRS, Immunoconcept, UMR 5164, 146 rue Léo Saignat, 33 076 Bordeaux, France

4. Department of Dermatology and Pediatric Dermatology, National Center for Rare Skin Disorders, Hôpital Saint André, 1 Rue Jean Burguet, 33 000 Bordeaux, France
5. Department of Cardiology, Hôpital Haut-Levêque, avenue de Magellan, 33 600 Pessac, France
6. Department of Vascular Medicine, Hôpital Saint André, 1 Rue Jean Burguet, 33 000 Bordeaux, France
7. Department of Internal Medicine, National Reference Center for Systemic Autoimmune Rare Diseases, Hôpital Haut-Levêque, avenue de Magellan, 33 600 Pessac, France

Corresponding author: Pauline Henrot – pauline.henrot@u-bordeaux.fr, Inserm U1035, Université de Bordeaux, 146 rue Léo Saignat, 33 076 Bordeaux, France – Tel: +33 5 57 57 13 73 / fax : +33 5 57 57 13 74

Short title: CCN3 role in SSc vasculopathy

Abbreviations: SSc: Systemic Sclerosis, NOV/CCN3: nephroblastoma overexpressed, HDMECs: human microvascular dermal endothelial cells

Word count: 3119, abstract word count: 182

Number of figures: 4, Number of tables: 1

Keywords: scleroderma, angiogenesis, tubulogenesis, NOV, CCN proteins

ABSTRACT

Systemic sclerosis (SSc) is a rare and severe connective tissue disease combining auto-immune and vasculopathy features, ultimately leading to organ fibrosis. Impaired angiogenesis is an often silent and life-threatening complication of the disease. We hypothesize that CCN3 (NOV), a member of the CCN family of extra-cellular matrix proteins, which is an antagonist of the pro-fibrotic protein CCN2 (CTGF) as well as a pro-angiogenic factor, is implicated in SSc pathophysiology.

We performed skin biopsies on 26 SSc patients, both in fibrotic and non-fibrotic areas for 17 patients, and collected 18 healthy control skin specimens, for immunohistochemistry and cell culture.

Histological analysis of non-fibrotic and fibrotic SSc skin shows a systemic decrease of papillary dermis surface as well as capillaries disappearance. CCN3 expression is systematically decreased in the dermis of SSc patients compared to healthy controls, particularly in dermal blood vessels. Moreover, CCN3 is decreased *in vitro* in endothelial cells from SSc patients. We show that CCN3 is essential for endothelial cell migration and angiogenesis *in vitro*.

In conclusion, CCN3 may represent a promising therapeutic target for SSc patients presenting with vascular involvement.

INTRODUCTION

Systemic sclerosis (SSc) is a rare and severe connective tissue disease combining autoimmunity and widespread vasculopathy, ultimately leading to organ fibrosis (Allanore et al. 2015; Gabrielli et al. 2009; Varga and Abraham 2007). Vasculopathy is a major issue in SSc (Allanore et al. 2018) and Raynaud's phenomenon is usually the first manifestation of the disease. Digital ulcers (DUs) are frequent in SSc patients, responsible for serious morbidity such as gangrene and amputation, and associated with higher mortality (Meunier et al. 2018). Other vasculopathic manifestations such as pulmonary hypertension or renal crisis are silent at an early stage but are potentially lethal. A current challenge lies in discovering new therapeutic targets in order to treat these manifestations.

CTGF (connective tissue growth factor), which is also known as CCN2, is a well-known pro-fibrotic factor in SSc (Leask et al. 2004; Serratì et al. 2013). CCN proteins, a family of six matricellular proteins sharing a common multimodular structure, are involved in major cellular pathways of interest in SSc (Henrot et al. 2018). CCN3 (NOV) is thought to be an antagonist of CCN2 when induced by TGF-β (Lemaire et al. 2010; Madne and Dockrell 2018; Riser et al. 2009). However, CCN3 is also pro-angiogenic, probably by binding to cell surface integrins such as integrin α5β1, α6β1 and αvβ5 (Lin et al. 2005). Interestingly, CCN3 has been shown to be decreased in the placenta of pre-eclampsia pregnant women, a disease whose pathophysiology mimics SSc renal crisis (Gellhaus 2006).

Thus, our hypothesis was that CCN3 could be a key player in SSc, particularly in vascular function. The aim of our work was to study the alteration of CCN3 in SSc skin and its role in SSc angiogenic dysfunction.

RESULTS

SSc skin is characterized by a major decrease in papillary dermis

Skin biopsies from 26 SSc patients were compared to 18 healthy control (HC) samples. Clinical characteristics of patients and controls are shown in Table 1. The thickness of the superficial (papillary) dermis was significantly decreased both in non-fibrotic (or clinically uninvolved) and fibrotic areas of SSc skin compared to HC skin (NFib: 0.0527 ± 0.006 mm, Fib: 0.0595 ± 0.006 mm; HC: 0.122 ± 0.008 mm; $p<0.0001$ in both cases; Figure 1a, b), even at the early stages of the disease (Figure 1a, recent SSc: <1 year of evolution after diagnosis). A significant decrease in the interdigitation index, representing a flattening of the basal membrane as compared to HC, was also noted both in non-fibrotic and fibrotic areas (HC: 1.76 ± 0.442; SSc NFib: 1.31 ± 0.264; SSc Fib: 1.35 ± 0.240; $p=0.0007$ and 0.002, respectively; Figure S1).

CD31 immunostaining (Figure 1c) showed a significant decrease in the number of dermal blood vessels in SSc skin, both in non-fibrotic and fibrotic areas compared to HC (NFib: 6.14 ± 0.927 dermal vessels/field, Fib: 6.66 ± 0.891 dermal vessels/field; HC: 23.5 ± 2.41 dermal vessels/field; $p<0.0001$ in both cases; Figure 1d). This was at least partly due to the disappearance of papillary dermal vessels (mainly capillaries), as evidenced by the significant decrease in the proportion of capillaries in non-fibrotic and fibrotic SSc skin versus HC (NFib: 62.7 ± 0.0597 %, Fib: 65 ± 0.0582 %; HC: 87.8 ± 0.0203 %; $p=0.0009$ and $p=0.0008$, respectively; Figure 1e).

SSc skin is characterized by a decrease in CCN3 expression in dermal vessels

Dermal vessels were then stained for CCN3 and CD34 (Figure 2a), the latter to evidence both endothelial cells (inner layer, white arrow) and peri-vascular CD34+ cells (outer layer, yellow

arrows) surrounding the dermal vessels. In HC samples, several layers of CCN3+ cells were observed: the CD34+/CCN3+ inner layer was identified as the tunica intima, the middle layer as the tunica media thanks to α-SMA staining (Figure S2), and the outer layer as CD34+/CCN3+ peri-vascular cells (Figure 2a). Other peri-vascular CCN3+ cells were identified as lymphocytes (CD3+) and fibroblasts (CD90+) (Figure S2).

We observed a marked decrease in the number of CD34/CCN3+ layers in SSc dermal vessels compared to HC ($p<0.0001$, Figure 2b), especially in reticular dermal vessels, which was mainly attributed to the loss of CD34+ peri-vascular cells. Of note, the number of CCN3+ layers did not differ regardless of the SSc skin area, fibrotic or not (Figure S3a).

We observed a marked decrease in CCN3 intensity in SSc endothelial cells (identified by CD31 staining) (1.58 ± 0.117 AU) compared to HC endothelial cells (2.71 ± 0.175 AU; $p<0.0001$, Figure 2c, d). Again, we observed no difference between non-fibrotic and fibrotic areas of SSc skin (Figure S3b). Of note, this result, as a mean CCN3 fluorescence intensity of all CD31+ cells, was neither influenced by the number nor by the size of dermal vessels. CCN3 expression in SSc endothelial cells did not differ in subgroup analysis regarding vascular involvement of SSc patients (Figure S3c). Interestingly, the mean CCN3 expression in endothelial cells was significantly correlated with the number of vessels (Spearman $r=0.6227$, $p<0.0001$, Figure S3d).

We also observed a significant decrease in dermal cell density in SSc skin compared to HC skin (data not shown), which partially accounts for the lack of other CCN3+ cells in the dermis as shown in Figure 2c. Of note, epidermal expression of CCN3 was not found different between HC and SSc, although great heterogeneity was observed among SSc samples (data not shown).

CCN3 level is decreased *in vitro* and CCN3 is differentially localized in SSc endothelial cells compared to HC cells

Cultured human microvascular dermal endothelial cells (HDMECs) from SSc biopsies and HC skin were checked for phenotype by CD31 labeling and flow cytometry (Figure 3a, Figure S4a). All cell populations (HC (n=7) and SSc (n=6)) were more than 95% CD31+. Western blotting revealed a significant decrease in intra-cellular CCN3 in SSc HDMECs compared to HC ones (p=0.04, Figure 3b and 3c). Of note, qPCR did not reveal any difference in CCN3 expression at the transcriptional level (Figure S4b).

CCN3 staining in HC HDMECs revealed both a cytoplasmic and nuclear expression, with a granulated peri-nuclear staining, suggesting an accumulation in the Golgi apparatus, as described elsewhere (Perbal 2006) (Figure 3d). Interestingly, intra-nuclear CCN3 staining was almost absent in SSc HDMECs, suggesting an intra-cytoplasmic retention of the protein. Moreover, the level of secreted CCN3 measured by ELISA in cell supernatants was significantly decreased in SSc HDMECs compared to HC HDMECs (p=0.01, Figure 3e). Secreted CCN3 was undetectable in 4 out of 5 SSc samples.

Altogether, these findings demonstrate that CCN3 is downregulated in SSc endothelial cells at both the intra-cellular and secreted level.

It is interesting to note that, although CCN3 basal secretion is very low in SSc HDMECs, it seems to be amenable to modulation. We have stimulated HC and SSc HDMECs with the pro-inflammatory cytokine IL-1β and found that CCN3 secretion tended to increase in SSc HDMECs only (Figure S5).

CCN3 is involved in HDMECs *in vitro* angiogenesis

In vitro angiogenesis assays showed that incubation of HDMECs with anti-CCN3 antibody significantly impaired tube formation compared to control antibody (Figure 4a and 4b). We observed a significant decrease in the number of master junctions (p=0.008), meshes (p=0.01) and master segments (p=0.01) (Figure 4c and 4d; Figure S6b). A significant decrease in the total length of master segments (p=0.01) and in the total segment length (p=0.02) (Figure 4e; Figure S6c) was also observed. The total length of isolated branches tended to increase in the presence of anti-CCN3 antibody compared to control antibody, without reaching statistical significance (Figure S6d). Definition of each parameter is shown in Figure S6a. No significant difference was observed between non-treated cells and HDMECs treated with control antibody (data not shown).

We sought to determine the mechanism underlying this impaired angiogenesis. The anti-CCN3 antibody had no significant effect on cell proliferation and cell adhesion compared to control antibody and to non-treated cells (Figure S7a, b). However, a significantly decreased migration was observed in HDMECs incubated with the anti-CCN3 antibody compared to the control condition (Figure S7c), as assessed by the level of wound closure 8 hours after the beginning of the experiment (p=0.02; Figure S7d). No significant difference was observed between the control isotypic antibody and non-treated cells (data not shown). Altogether, these findings show that CCN3 blockade in HC HDMECs impairs *in vitro* angiogenesis at least partly by inhibiting migration.

Next, we incubated SSc HDMECs with various doses of recombinant CCN3 (rCCN3: 0.1, 1 and 10 µg/mL). rCCN3 0.1 and 1 µg/mL showed a tendency to improve *in vitro* angiogenesis, although not statistically significant (data not shown). rCCN3 10 µg/mL significantly improved *in vitro* angiogenesis, as shown by the significant increase in the number of master

junctions (p=0.0066; Figure 4h) and the number of meshes (p=0.0097; Figure 4i). A significant increase in the number of master segments (p=0.0005, Figure S6e) and the total segment length (p=0.0066, Figure S6f) was also observed. Finally, the total length of isolated branches tended to decrease in presence of rCCN3 (Figure S6g). Addition of rCCN3 (10 µg/mL) to SSc HDMECs in a migration assay did not significantly change the level of wound closure (Figure S7 e, f).

Altogether, these data show that rCCN3 partly restores the angiogenesis defect observed in SSc HDMECs.

DISCUSSION

Our results highlight a systemic architectural modification in SSc skin, as shown by the loss of papillary dermis and capillaries. These changes are associated with a global downregulation of CCN3 in dermal vessels and endothelial cells. CCN3 was found to play a prominent role in HDMECs migration and angiogenesis *in vitro*.

One striking histological finding was the disappearance of papillary dermis, seen whatever the area of biopsy in SSc skin, as mirrored by a dramatic decrease in the number of capillaries. Comparison of the same clinical sites that we analyzed (dorsal forearm and upper inner arm) also found similar histological features between the two zones (Van Praet et al. 2011). Of note, studies analyzing fibroblasts taken from both non-fibrotic and fibrotic zones in the same patients have either shown a difference in the molecular patterns (Corallo et al. 2017) or no difference (Fuzii et al. 2008). This decrease in papillary dermal surface seems to be different than papillary changes observed in other dermatological conditions such as lichen sclerosus et atrophicus, where the papillary dermis is often edematous (Brănişteanu et al. 2016; Uitto et al. 1980). In any case, there is a need to decipher the pathophysiological mechanism behind the selective destruction of papillary dermis. It could be due to the enhanced secretion of matrix metallo-proteinases by inflammatory cells or to tissular destruction by local hypoxia in the context of SSc-impaired angiogenesis.

Inflammation and hypoxia are factors that modulate the level of CCN proteins, in particular CCN3 (Jun and Lau 2011; Wolf et al. 2010). We observed a decreased dermal protein level of CCN3 *in situ* in the skin of SSc patients. This result is not in contradiction with the increase in CCN3 found by Lemaire et al (Lemaire et al. 2010), since they analyzed whole skin samples at the transcriptional level. The high rate of post-translational modifications of CCN3 (Kyurkchiev et al. 2004; Yang et al. 2011) demonstrates the need for assessment at the protein

level, as shown by the discrepancy between qPCR and Western blot results in our work. Here, degradation of CCN3 protein in SSc HDMECs could be enhanced, or CCN3 stabilization (through dimerization for example) could be decreased. Moreover, we found CD34+/CCN3+ perivascular cells in HC skin that were almost absent in SSc skin. Due to the expression of CD34, the peri-vascular localization and peculiar morphological characteristics (small cell body and long cytoplasmic prolongations), these cells could either be telocytes which have been reported as decreased in SSc skin (Manetti et al. 2013), or mesenchymal stem cells (Barron et al. 2019). The origin of these CD34+ peri-vascular cells remains unclear, yet their loss contributes to the decrease of CCN3 expression in dermal vessels.

We show that CCN3 blockade impairs HC HDMECs *in vitro* angiogenesis, and that adding recombinant CCN3 to SSc HDEMCs improves *in vitro* angiogenesis. These results are consistent with the impaired *in vitro* angiogenesis already observed in SSc endothelial cells compared to HC cells (Tsou et al. 2016). Thus, CCN3 seems to play a prominent role in HDMECs homeostasis, which is consistent with other reports (Lin et al. 2003; van Roeyen et al. 2012). In SSc HDMECs, low CCN3 expression seems to be amenable to modulation by stimulation with IL-1β (whereas no change in CCN3 extra-cellular secretion was seen in HC cells), although these data need to be confirmed with a larger data set. IL-1β stimulation activates many pathways in endothelial cells, triggering a response program including potent pro-angiogenic factors, notably via NF-κB pathway (Pober and Sessa 2007). These data could lead to decipher the IL-1β/CCN3 axis in endothelial cells on a therapeutic prospect.

Impaired tube formation can be due to decreased migration or dysfunction in cell-cell attachment (Irvin et al. 2014). This is consistent with our results, showing a more important decrease of tube formation than in migration. This cannot be attributed to a difference in cell proliferation, given that it was not altered by anti-CCN3 treatment. Thus, in our model, CCN3 blockade probably impairs mostly cell-cell attachment through defect in integrin binding,

directly or indirectly. A direct interaction between CCN3 and endothelial cells surface integrins (αVβ3, α6β1, α5β1) has indeed already been shown (Lin et al. 2005; Lin et al. 2003). CCN3 blockade could also impair CCN3's binding to extra-cellular matrix (ECM) constituents (LIU et al. 2012) and thus inhibiting tubulogenesis by preventing ECM degradation. Adding rCCN3 to SSc HDMECs partly restores *in vitro* angiogenesis, which is particularly interesting from a therapeutic point of view.

However, the full role of CCN3 in endothelial cells remains unknown. Intra-cellular CCN3, and particularly the nuclear form, may act as a co-transcriptional factor to regulate angiogenesis as well as other cellular functions. We have shown that SSc HDMECs do not exhibit intra-nuclear CCN3 staining, unlike healthy HDMECs. Further studies are needed to fully understand if intra-nuclear CCN3 regulates HDMECs homeostasis.

Altogether, our data suggests the involvement of CCN3 in SSc skin pathophysiology, especially vasculopathy. On another note, CCN3 has been reported as antagonizing the pro-fibrotic role of CCN2 in several models (Borkham-Kamphorst et al. 2012; Lafont et al. 2005; Lemaire et al. 2010; Riser et al. 2009) but not in the skin. Here, we show that CCN3 plays a pro-angiogenic role, CCN2 also being reported as a pro-angiogenic factor (Brigstock 2002; Chintala et al. 2012; Ponticos 2013). It is likely that CCN3's role is organ and function-dependant and its anti-fibrotic role in the skin remains to be demonstrated.

In conclusion, our results indicate that decrease of CCN3 in SSc endothelial cells is linked to SSc impaired angiogenesis. A future challenge is to develop therapeutic approaches to restore CCN3 homeostasis in the skin.

MATERIALS AND METHODS

Patients and controls

26 SSc patients were recruited within the biomedical research cohort VISS (Vasculopathy and Inflammation in Systemic Sclerosis) approved by the institutional ethical committee (CPP, 2012 A00081-42, Aquitaine), over a two-year period (from September 2015 to September 2017). All patients met the classification criteria proposed by the American College of Rheumatology (ACR) and the EUropean League Against Rheumatism (EULAR) 2013 (26). All patients provided written, informed consent before entering the study. Skin biopsies were performed on the forearm, on a fibrotic zone whenever possible, as spindle-shaped biopsies of 1 cm of wide axis. If the forearm was fibrotic (17 patients), another similar biopsy was performed on the proximal part of the same arm, in a non-fibrotic zone. For healthy control (HC) skin, 18 biopsy specimens were isolated from arm skin that had been discarded during plastic surgery (brachioplasty) thanks to a research convention with the plastic surgery department. For SSc patients, vascular involvement was defined as current or past history of digital ulcers and/or pulmonary hypertension and/or renal crisis.

Histological assessment, immunohistochemistry, immunofluorescence

Part of the skin biopsy was formalin-fixed and paraffin-embedded before undergoing 4µm-thick microtome sections, another part being devoted for cell culture. Histological analyses were performed using Masson's Trichrome Aniline Blue staining. Immunohistochemistry (IHC) was performed as previously described (Cario-Andre 2017; Marie et al. 2014), using antibodies against CCN3 (ab137677; Abcam), CD31 (clone JC70A; Dako), CD34 (QBEnd-10; Thermo Fisher Scientific). Same dilutions were used for all immunohistochemical stains.

Images were acquired using an epifluorescence microscope (Leica). For analysis, see supplemental material & methods.

Endothelial cell primary cell culture

Human microvascular dermal endothelial cells (HDMECs) were obtained from 5 SSc patients and 7 HC skin samples, based on a previous protocol(Normand and Karasek 1995), improved with purification using a CD31 microbead kit (Miltenyi). The cells were then cultured in MV2 EC medium (Promocell) and used between passages 2 and 5.

Flow cytometry

One passage after purification, HDMECs were labeled with an APC anti-CD31 (clone AC128, Miltenyi). Cells were analyzed using Canto I flow cytometer with FACSDiva software (BD) and data analysis was performed with FlowJo 10.1 software.

Immunocytochemistry

Cultured cells were fixed in 4% formol, washed with PBS, permeabilized with PBS-TritonX100 0.2%, saturated with FCS 2.5% and incubated overnight (4°C) with anti-CCN3 (ab137677; Abcam). Images were acquired using an epifluorescence microscope (Nikon Eclipse).

Western blotting

Cells were scraped with RIPA buffer and lysates were centrifuged 20min at 12500 rpm, 4°C. After electrophoresis on a 10% acrylamide gel, proteins were transferred to a PVDF membrane. Membranes were saturated in TBS-5% milk, then incubated with antibodies against CCN3 (ab191425; Abcam), β-actin (Sigma), and corresponding secondary antibodies

(Vector Laboratories) and revealed with ECL+ (Amersham). Chemiluminescence acquisitions were performed using LAS-3000 Reader (Fujifilm Life Science). Quantification analyses were performed using ImageLab 6.0 software (Bio-Rad Laboratories).

Determination of secreted CCN3 level

CCN3 levels in serum and cell culture supernatants were quantified using an ELISA kit (R&D Systems), according to the manufacturer's instructions. The cut-off for CCN3 positivity was defined as values equal or superior to 8 pg/ml, which corresponds to the detection limit of the ELISA.

Angiogenesis assay

HDMECs from three different healthy and SSc donors were seeded on 6-well plates (200 000 cells/well) and after allowing them to adhere, were incubated overnight with either 0.5 µg/mL of anti-CCN3 (ab137677; Abcam) or control antibody (ab37415; Abcam), either recombinant CCN3 (0.1, 1 or 10 µg/mL) (120-26; PeproTech). The day after, cells were seeded in complete growth medium MV2 on Ibidi microslides (Ibidi, cat. No. 81506) coated with Matrigel Matrix Growth Factor Reduced, Phenol Red-Free (BD, cat. No. 356231) and allowed to form tubes at 37°C. 10 000 cells were used per well, 5 wells were used per condition in a single experiment and experiments were replicated three times. Pictures were taken 6 and 24 hours after the beginning of the experiment with a phase contrast microscope (Leica). For analysis, see supplementary material & methods.

For supplementary figures, see supplementary material & methods.

Data Availability Statement

No datasets were generated or analyzed during the current study.

Conflict of interest

TS: Abbvie: advice, consultancy, clinical trials; Lilly: advice, consultancy, clinical trials; Pfizer: advice, consultancy, research grant; Novartis: advice, clinical trials, Abivax: clinical trials; Biogen: clinical trials. The other authors state no conflict of interest.

Acknowledgements

This work was funded by Fédération de Recherche Transbiomed, Association des Sclérodermiques de France and Société Française de Dermatologie. The authors wish to thank Sébastien Marais, from the Bordeaux Imaging Center, for his precious help concerning ImageJ analysis, Catherine Pain, for technical assistance, and all the clinicians (Claire Carcaud, Gaël Galli) and patients who took part in the VISS cohort.

CRediT statement

Conceptualization and writing – original draft: PH, MET, FM and MC; investigation: PH, PL, PM, VJ, and VL; formal analysis: PH; funding acquisition: PH, MET and MC; resources: FM, PKC, FP, CB, TS, JS, and EL; supervision: MET, FM, HRR, AT and MC; visualization: PH and MET; writing- review and editing: PH, FM, MET and MC. All authors read and approved the final manuscript.

REFERENCES

Allanore Y, Distler O, Matucci-Cerinic M, Denton CP. Review: Defining a Unified Vascular Phenotype in Systemic Sclerosis. Arthritis & Rheumatology (Hoboken, N.J.). 2018;70(2):162–70

Allanore Y, Simms R, Distler O, Trojanowska M, Pope J, Denton CP, et al. Systemic sclerosis. Nat Rev Dis Primers. 2015;1:15002

Barron AMS, Mantero JC, Ho JD, Nazari B, Horback KL, Bhawan J, et al. Perivascular Adventitial Fibroblast Specialization Accompanies T Cell Retention in the Inflamed Human Dermis. J. Immunol. 2019;202(1):56–68

Borkham-Kamphorst E, Huss S, Van de Leur E, Haas U, Weiskirchen R. Adenoviral CCN3/NOV gene transfer fails to mitigate liver fibrosis in an experimental bile duct ligation model because of hepatocyte apoptosis. Liver Int. 2012;32(9):1342–53

Brănişteanu DE, Brănişteanu DC, Stoleriu G, Ferariu D, Voicu CM, Stoica LE, et al. Histopathological and clinical traps in lichen sclerosus: a case report. Rom J Morphol Embryol. 2016;57(2 Suppl):817–23

Brigstock DR. Regulation of angiogenesis and endothelial cell function by connective tissue growth factor (CTGF) and cysteine-rich 61 (CYR61). Angiogenesis. 2002;5(3):153–65

Cario-Andre M. Analysis of CCN Expression by Immunofluorescence on Skin Cells, Skin, and Reconstructed Epidermis. Methods Mol. Biol. 2017;1489:63–76

Chintala H, Liu H, Parmar R, Kamalska M, Kim YJ, Lovett D, et al. Connective tissue growth factor regulates retinal neovascularization through p53 protein-dependent transactivation of the matrix metalloproteinase (MMP)-2 gene. J. Biol. Chem. 2012;287(48):40570–85

Corallo C, Santucci A, Bernardini G, Figura N, Leoncini R, Riolo G, et al. Proteomic Investigation of Dermal Fibroblasts Isolated from Affected and Unaffected Skin Samples from Patients with Limited Cutaneous Systemic Sclerosis: 2 Distinct Entities? J. Rheumatol. 2017;44(1):40–8

Fuzii HT, Yoshikawa GT, Junta CM, Sandrin-Garcia P, Fachin AL, Sakamoto-Hojo ET, et al. Affected and non-affected skin fibroblasts from systemic sclerosis patients share a gene expression profile deviated from the one observed in healthy individuals. Clin Exp Rheumatol. 2008;26(5):866–74

Gabrielli A, Avvedimento EV, Krieg T. Scleroderma. N. Engl. J. Med. 2009;360(19):1989–2003

Gellhaus A. Decreased expression of the angiogenic regulators CYR61 (CCN1) and NOV (CCN3) in human placenta is associatedwith pre-eclampsia. Molecular Human Reproduction. 2006;12(6):389–99

Henrot P, Truchetet M-E, Fisher G, Taïeb A, Cario M. CCN proteins as potential actionable targets in scleroderma. Exp. Dermatol. 2018;

van den Hoogen F, Khanna D, Fransen J, Johnson SR, Baron M, Tyndall A, et al. 2013 classification criteria for systemic sclerosis: an American College of Rheumatology/European League against Rheumatism collaborative initiative. Arthritis Rheum. 2013;65(11):2737–47

Irvin MW, Zijlstra A, Wikswo JP, Pozzi A. Techniques and assays for the study of angiogenesis. Exp Biol Med (Maywood). 2014;239(11):1476–88

Jun J-I, Lau LF. Taking aim at the extracellular matrix: CCN proteins as emerging therapeutic targets. Nature Reviews Drug Discovery. 2011;10(12):945–63

Kyurkchiev S, Yeger H, Bleau A-M, Perbal B. Potential cellular conformations of the CCN3(NOV) protein. Cell Commun Signal. 2004;2:9

Lafont J, Jacques C, Le Dreau G, Calhabeu F, Thibout H, Dubois C, et al. New target genes for NOV/CCN3 in chondrocytes: TGF-beta2 and type X collagen. J. Bone Miner. Res. 2005;20(12):2213–23

Leask A, Denton CP, Abraham DJ. Insights into the molecular mechanism of chronic fibrosis: the role of connective tissue growth factor in scleroderma. J. Invest. Dermatol. 2004;122(1):1–6

Lemaire R, Farina G, Bayle J, Dimarzio M, Pendergrass SA, Milano A, et al. Antagonistic effect of the matricellular signaling protein CCN3 on TGF-beta- and Wnt-mediated fibrillinogenesis in systemic sclerosis and Marfan syndrome. J. Invest. Dermatol. 2010;130(6):1514–23

Lin CG, Chen C-C, Leu S-J, Grzeszkiewicz TM, Lau LF. Integrin-dependent functions of the angiogenic inducer NOV (CCN3): implication in wound healing. J. Biol. Chem. 2005;280(9):8229–37

Lin CG, Leu S-J, Chen N, Tebeau CM, Lin S-X, Yeung C-Y, et al. CCN3 (NOV) Is a Novel Angiogenic Regulator of the CCN Protein Family. Journal of Biological Chemistry. 2003;278(26):24200–8

LIU S, LIU Z, BI D, YUAN X, LIU X, DING S, et al. CCN3 (NOV) regulates proliferation, adhesion, migration and invasion in clear cell renal cell carcinoma. Oncol Lett. 2012;3(5):1099–104

Madne TH, Dockrell MEC. CCN3, a key matricellular protein, distinctly inhibits TGFβ1-mediated Smad1/5/8 signalling in human podocyte culture. Cell. Mol. Biol. (Noisy-le-grand). 2018;64(3):5–10

Manetti M, Guiducci S, Ruffo M, Rosa I, Faussone-Pellegrini MS, Matucci-Cerinic M, et al. Evidence for progressive reduction and loss of telocytes in the dermal cellular network of systemic sclerosis. J. Cell. Mol. Med. 2013;17(4):482–96

Marie J, Kovacs D, Pain C, Jouary T, Cota C, Vergier B, et al. Inflammasome activation and vitiligo/nonsegmental vitiligo progression. Br. J. Dermatol. 2014;170(4):816–23

Meunier P, Dequidt L, Barnetche T, Lazaro E, Duffau P, Richez C, et al. Increased risk of mortality in systemic sclerosis-associated digital ulcers: a systematic review and meta-analysis. J Eur Acad Dermatol Venereol. 2018;

Normand J, Karasek MA. A method for the isolation and serial propagation of keratinocytes, endothelial cells, and fibroblasts from a single punch biopsy of human skin. In Vitro Cell. Dev. Biol. Anim. 1995;31(6):447–55

Perbal B. New insight into CCN3 interactions - Nuclear CCN3 : fact or fantasy? Cell Commun Signal. 2006;4:6

Pober JS, Sessa WC. Evolving functions of endothelial cells in inflammation. Nat. Rev. Immunol. 2007;7(10):803–15

Ponticos M. Connective tissue growth factor (CCN2) in blood vessels. Vascul. Pharmacol. 2013;58(3):189–93

Riser BL, Najmabadi F, Perbal B, Peterson DR, Rambow JA, Riser ML, et al. CCN3 (NOV) is a negative regulator of CCN2 (CTGF) and a novel endogenous inhibitor of the fibrotic pathway in an in vitro model of renal disease. Am. J. Pathol. 2009;174(5):1725–34

van Roeyen CRC, Boor P, Borkham-Kamphorst E, Rong S, Kunter U, Martin IV, et al. A novel, dual role of CCN3 in experimental glomerulonephritis: pro-angiogenic and antimesangioproliferative effects. Am. J. Pathol. 2012;180(5):1979–90

Serratì S, Chillà A, Laurenzana A, Margheri F, Giannoni E, Magnelli L, et al. Systemic sclerosis endothelial cells recruit and activate dermal fibroblasts by induction of a connective tissue growth factor (CCN2)/transforming growth factor β-dependent mesenchymal-to-mesenchymal transition. Arthritis & Rheumatism. 2013;65(1):258–69

Tsou P-S, Wren JD, Amin MA, Schiopu E, Fox DA, Khanna D, et al. Histone Deacetylase 5 is Overexpressed in Scleroderma Endothelial Cells and Impairs Angiogenesis via Repressing Pro-angiogenic Factors. Arthritis Rheumatol. 2016;68(12):2975–85

Uitto J, Santa Cruz DJ, Bauer EA, Eisen AZ. Morphea and lichen sclerosus et atrophicus. Clinical and histopathologic studies in patients with combined features. J. Am. Acad. Dermatol. 1980;3(3):271–9

Van Praet JT, Smith V, Haspeslagh M, Degryse N, Elewaut D, De Keyser F. Histopathological cutaneous alterations in systemic sclerosis: a clinicopathological study. Arthritis research & therapy. 2011;13(1):1

Varga J, Abraham D. Systemic sclerosis: a prototypic multisystem fibrotic disorder. J. Clin. Invest. 2007;117(3):557–67

Wolf N, Yang W, Dunk CE, Gashaw I, Lye SJ, Ring T, et al. Regulation of the matricellular proteins CYR61 (CCN1) and NOV (CCN3) by hypoxia-inducible factor-1{alpha} and transforming-growth factor-{beta}3 in the human trophoblast. Endocrinology. 2010;151(6):2835–45

Yang W, Wagener J, Wolf N, Schmidt M, Kimmig R, Winterhager E, et al. Impact of CCN3 (NOV) glycosylation on migration/invasion properties and cell growth of the choriocarcinoma cell line Jeg3. Hum. Reprod. 2011;26(10):2850–60

TABLES

		SSc patients (n=26)	Healthy controls (n=18)	
Demographic characteristics	Age (yo): mean (SD)	58.88 (9.45)	47.29 (9.85)	p=0.0005
	Female: n (%)	15 (53.8)	16 (88.9)	p=0.1037
	DcSSc: n (%)	10 (38)		
	Disease duration (y): mean (SD)	5.69 (5.46)		
Cutaneous involvement	mRSS: mean (SD)	16.5 (12)		
	Pigmentary disorders: n (%)	14 (54)		
Vascular involvement	Digital ulcers: n (%)	16 (62)		
	PAH: n (%)	4 (15)		
	SSc renal crisis: n (%)	1 (0.03)		
Pulmonary involvement	ILD: n (%)	11 (42)		
	Pulmonary fibrosis	3 (12)		
Gastro-intestinal involvement	Esophageal involvement: n (%)	19 (73)		
	Intestinal involvement: n (%)	3 (12)		
Musculo-skeletal involvement	Synovitis: n (%)	8 (30)		
	Joint contractures: n (%)	4 (15)		

Table 1: Characteristics of SSc patients and controls.

yo: years old, SD: standard deviation, DcSSc: diffuse cutaneous SSc, mRSS: modified Rodnan skin score, PAH: pulmonary arterial hypertension, ILD: interstitial lung disease.

FIGURE LEGENDS

Figure 1: Morphological changes in Systemic Sclerosis (SSc) dermis compared to healthy controls (HC). Apparently non-fibrotic SSc skin (NFib, or clinically uninvolved skin) displays histological changes similar to fibrotic (Fib, involved) skin.

Data represent mean ± SEM and are normalized by dermis surface. Each dot represents a patient or a HC sample (mean of three experiments for each dot). HC: n=18, SSc: n=26 (both zones for 17 patients).

a: Masson's Trichrome staining visualizing collagen fibers (blue). Top, healthy control arm; bottom, SSc arm (disease <1 year), non-fibrotic zone and fibrotic zone of the same patient (magnification x20). Scale bar, 50µm. White dots represent the junction between papillary (superficial) and reticular (deep) dermis.

b: Major decrease in papillary dermis thickness in SSc patients, both in non-fibrotic and fibrotic zones ($p<0.0001$).

c: Top, healthy control arm; bottom, SSc arm, non-fibrotic zone and fibrotic zone of the same patient (CD31/DAPI staining). White dots mark limit between epidermis and dermis. Magnification x40; scale bar, 50 µm.

d: Significant decrease in number of dermal vessels in SSc patients (counted thanks to CD31 staining). HC versus SSc Fib: $p<0.0001$; HC versus SSc NFib: $p<0.0001$.

e: Loss of small capillaries (papillary dermal vessels) in SSc skin. HC versus SSc Fib: $p=0.0008$; HC versus SSc NFib: $p=0.0009$.

Figure 2: CCN3 expression *in situ* in the dermis of SSc patients (n= 26) and HC (n=18). CCN3 is decreased in SSc patients' dermal vessels.

Data represent mean ± SEM of a minimum of three independent experiments. Representative pictures are shown.

a: CCN3/CD34 immunofluorescent staining of HC and SSc skin. CD34+ cells are endothelial cells (inner layer, white arrows, red dots) and surrounding peri-vascular CD34+ cells (outer layer, yellow arrow, yellow dots). Two layers of CD34+/CCN3+ cells can be seen in HC skin (top) whereas a single layer of CD34+/CCN3+ cells can be seen in SSc skin (bottom). Scale bar, 20µm.

b: Significant decrease in number of CCN3+ layers around dermal reticular vessels in SSc patients ($p<0.0001$, Mann-Whitney).

c: CCN3/CD31 immunofluorescent staining of HC and SSc skin. CD31+ cells are endothelial cells. CCN3 intensity is decreased in SSc CD31+ cells (bottom) compared to HC cells (top). Scale bar, 20µm.

d: Major decrease in CCN3 expression in endothelial cells of SSc dermal vessels compared to healthy controls ($p<0.0001$). MFI=mean fluorescence intensity.

HC vs SSc Nfib or Fib: unpaired t-tests with Welch's correction or Mann-Whitney when indicated; SSc Nfib vs Fib: paired t-tests.

Figure 3: CCN3 expression is decreased *in vitro* in cultured endothelial cells of SSc patients compared to HC.

a: Purity of human microvascular dermal endothelial cells (HDMECs) grown from SSc skin. Flow cytometry after staining for CD31 (APC) shows 98.2% of selected CD31+ population.

b, c: Significant decrease in CCN3 expression in SSc endothelial cells (HDMECs) (n=4) *in vitro* compared to healthy controls (n=7) (Western blot) ($p=0.0445$, unpaired t-test with Welch's correction). β-actin is shown as loading control. Results are mean of three experiments. Data represent mean ± SD. One representative experiment is shown.

d: Immunocytochemistry of CCN3 (green) in HC and SSc HDMECs. CCN3 can be found in cytoplasmic granules in both types of cells, but intra-nuclear staining is mostly seen in HC HDMECs and absent from SSc HDMECs. Representative pictures of two experiments involving six HC and six SSc patients are shown. Scale bar, 100 µm; close-up: scale bar, 20 µm.

e: Decrease in secreted CCN3 of SSc endothelial cells (HDMECs) (n=5) *in vitro* compared to healthy controls (n=5) (assessed by ELISA) (p=0.0159, Mann-Whitney). SN=supernatant. Data represent mean ± SD. Experiment was performed in triplicate.

Figure 4: CCN3 is involved in HDMECs *in vitro* angiogenesis. NT = non-treated cells; Ab = antibody, rCCN3 = recombinant CCN3. Each experiment was performed in quintuplicate. Data represent mean ± SEM of three independent experiments involving three different donors (for both HC and SSc cells). Representative pictures of one experiment are shown. Scale bar, 200 µm.

Panels a to e represent CCN3 blockade in HC HDMECs; panels f to j represent CCN3 addition to SSc HDMECs.

a: Angiogenesis assay on matrigel of HC HDMECs treated with control antibody. Pictures taken 24 hours after beginning of experiment (left panel). Analysis of tube number and quality shows master junctions as blue dots circled in red, master segments in yellow (right panel; software: angiogenesis analyzer for ImageJ).

b: Angiogenesis assay on matrigel of HC HDMECs treated with anti-CCN3 antibody. Pictures taken 24 hours after beginning of experiment (left panel).

c: Significant decrease in number of master junctions in HC HDMECs treated with anti-CCN3 compared to control antibody (p=0.0080).

d: Significant decrease in number of meshes in HC HDMECs treated with anti-CCN3 compared to control antibody (p=0.0146).

e: Significant decrease in total length of master segments in HC HDMECs treated with anti-CCN3 compared to control antibody (p=0.0104).

f: Angiogenesis assay on matrigel of untreated SSc HDMECs. Pictures taken 6 hours after beginning of experiment (left panel). Analysis of tube number and quality shows master junctions as blue dots circled in red, master segments in yellow (right panel; software: angiogenesis analyzer for ImageJ).

g: Angiogenesis assay on matrigel of SSc HDMECs treated with recombinant CCN3 (rCCN3) (10 µg/mL). Pictures taken 6 hours after beginning of experiment (left panel).

h: Significant increase in number of master junctions in SSc HDMECs treated with rCCN3 compared to untreated cells (p=0.0066).

i: Significant increase in number of meshes in SSc HDMECs treated with rCCN3 compared to untreated cells (p=0.0097).

j: Tendancy to increase in total length of master segments in SSc HDMECs treated with rCCN3 compared to untreated cells (p=0.0569).

Two-way ANOVA with Sidak's multiple comparisons test was performed for all analysis.

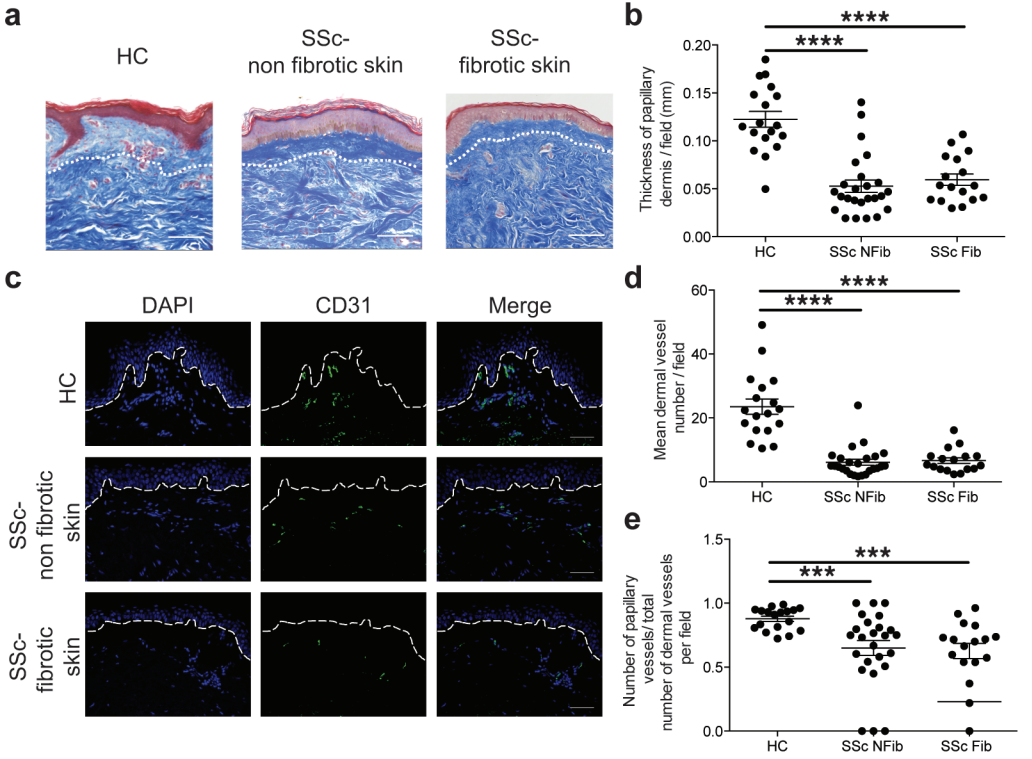
a
HC
SSc-
non fibrotic skin
SSc-
fibrotic skin
b
****
****
Thickness of papillary dermis / field (mm)
0.20
0.15
0.10
0.05
0.00
HC
SSc NFib
SSc Fib
c
DAPI
CD31
Merge
HC
SSc-
non fibrotic
skin
SSc-
fibrotic
skin
d
****
****
Mean dermal vessel number / field
60
40
20
0
HC
SSc NFib
SSc Fib
e
***
***
Number of papillary vessels/total number of dermal vessels per field
1.5
1.0
0.5
0.0
HC
SSc NFib
SSc Fib

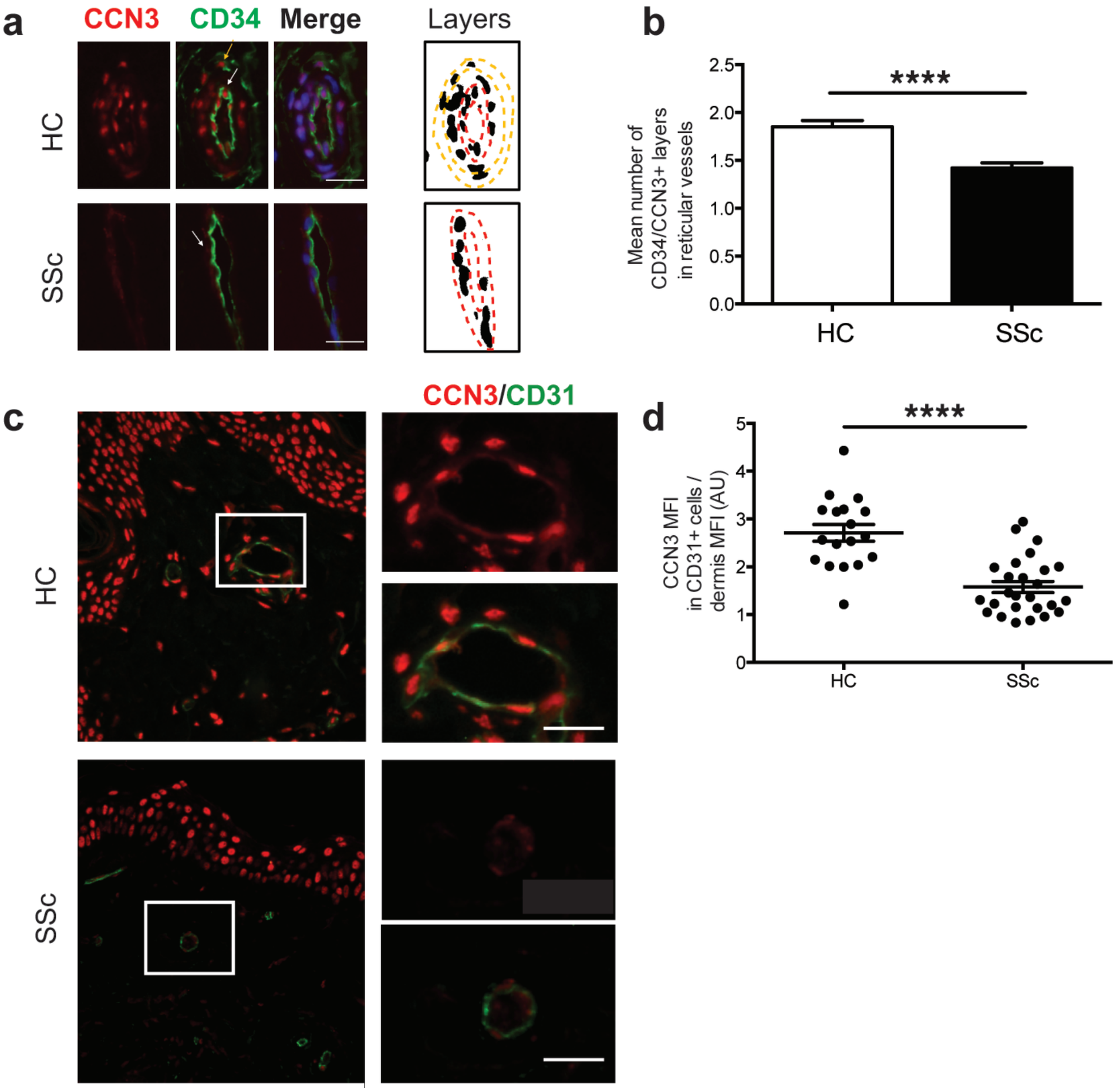
a
CCN3
CD34
Merge
Layers
HC
SSc
b
Mean number of CD34/CCN3+ layers in reticular vessels
2.5
2.0
1.5
1.0
0.5
0.0
****
HC
SSc
c
CCN3/CD31
HC
SSc
d
CCN3 MFI in CD31+ cells / dermis MFI (AU)
5
4
3
2
1
0
****
HC
SSc

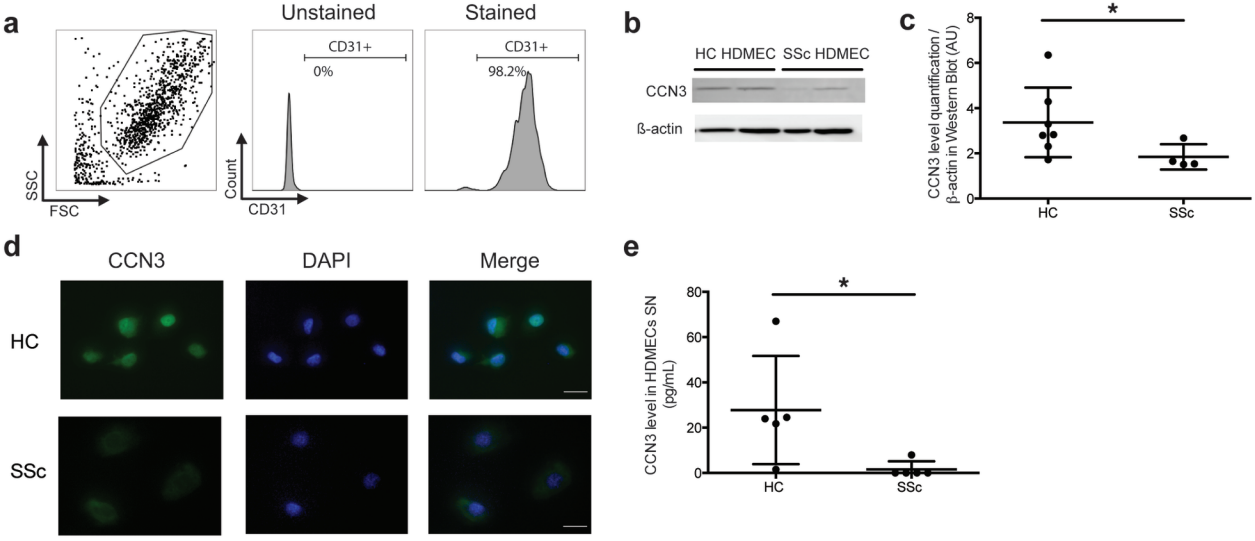
a
Unstained
Stained
CD31+
0%
CD31+
98.2%
SSC
FSC
Count
CD31
b
HC HDMEC
SSc HDMEC
CCN3
ß-actin
c
CCN3 level quantification / β-actin in Western Blot (AU)
HC
SSc
d
CCN3
DAPI
Merge
HC
SSc
e
CCN3 level in HDMECs SN (pg/mL)
HC
SSc

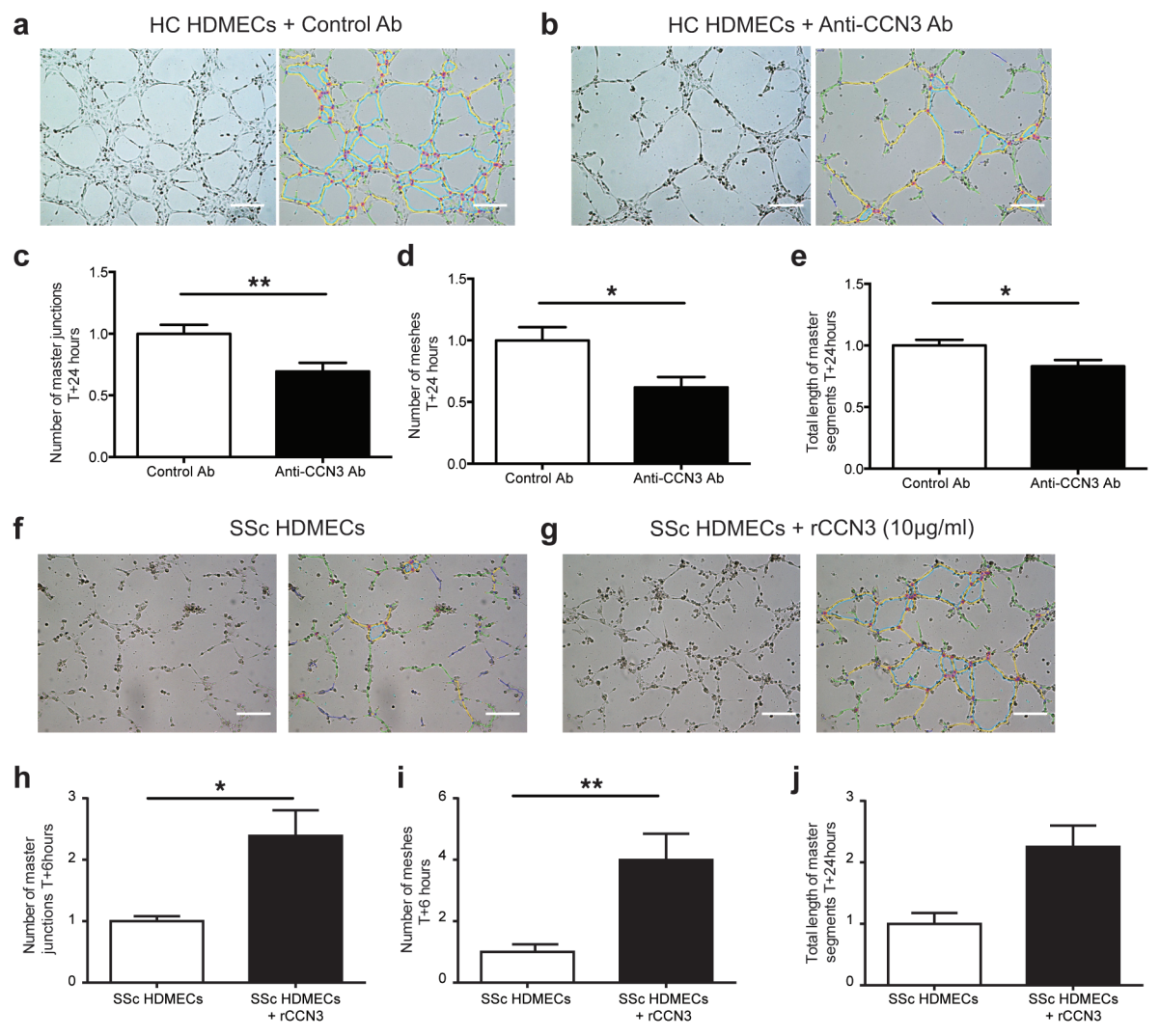
a
HC HDMECs + Control Ab
b
HC HDMECs + Anti-CCN3 Ab
c
Number of master junctions T+24 hours
1.5
1.0
0.5
0.0
**
Control Ab
Anti-CCN3 Ab
d
Number of meshes T+24 hours
1.5
1.0
0.5
0.0
*
Control Ab
Anti-CCN3 Ab
e
Total length of master segments T+24hours
1.5
1.0
0.5
0.0
*
Control Ab
Anti-CCN3 Ab
f
SSc HDMECs
g
SSc HDMECs + rCCN3 (10µg/ml)
h
Number of master junctions T+6hours
3
2
1
0
*
SSc HDMECs
SSc HDMECs + rCCN3
i
Number of meshes T+6 hours
6
4
2
0
**
SSc HDMECs
SSc HDMECs + rCCN3
j
Total length of master segments T+24hours
3
2
1
0
SSc HDMECs
SSc HDMECs + rCCN3

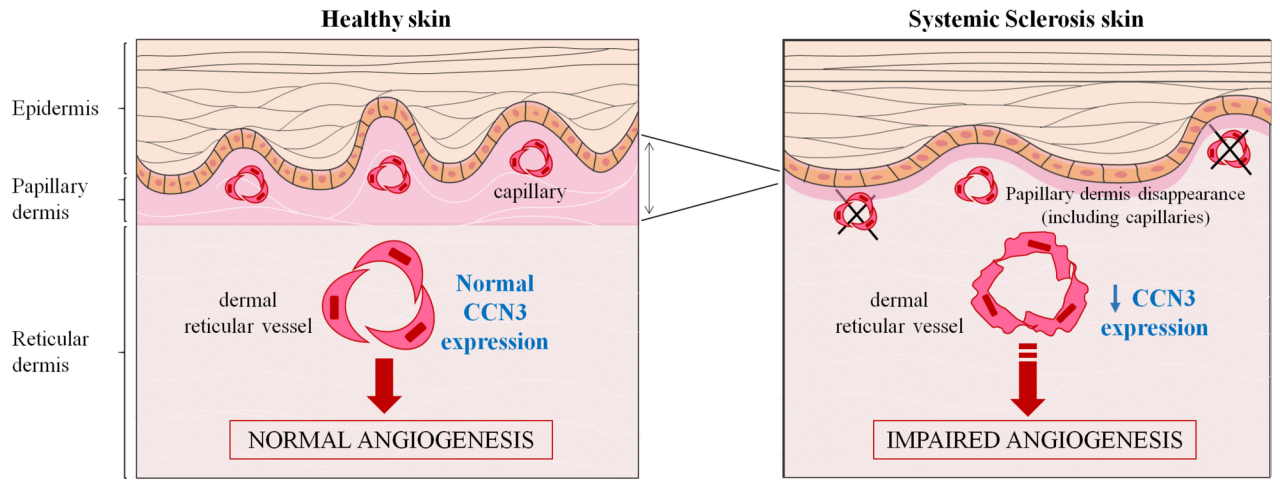
Healthy skin
Systemic Sclerosis skin
Epidermis
Papillary dermis
Reticular dermis
capillary
dermal reticular vessel
Normal CCN3 expression
NORMAL ANGIOGENESIS
Papillary dermis disappearance (including capillaries)
dermal reticular vessel
↓ CCN3 expression
IMPAIRED ANGIOGENESIS